Progress in PHOTOVOLTAICS

PROGRESS IN PHOTOVOLTAICS: RESEARCH AND APPLICATIONS
Prog. Photovolt: Res. Appl. 2014; **22**:949–957
Published online 18 February 2013 in Wiley Online Library (wileyonlinelibrary.com). DOI: 10.1002/pip.2346

RESEARCH ARTICLE

Change in *I–V* characteristics of thin-film photovoltaic (PV) modules induced by light soaking and thermal annealing effects

Tetsuyuki Ishii*, Kenji Otani, Takumi Takashima and Kazuaki Ikeda

Research Center for Photovoltaic Technologies, National Institute of Advanced Industrial Science and Technology (AIST), 1-1-1 Umezono, Tsukuba, Ibaraki 305-8568, Japan

ABSTRACT

The performance of photovoltaic (PV) modules is generally rated under standard test conditions (STC). However, the performance of thin-film photovoltaic modules is not unique even under STC, because of the "metastability". The effects of the light soaking and thermal annealing shall be incorporated into an appropriate energy rating standard. In this study, the change in *I–V* characteristics of thin-film PV modules caused by the metastability was examined by repeated indoor measurements in addition to round-robin outdoor measurements. The investigated thin-film modules were copper indium gallium (di)selenide (CIGS), a-Si : H, and a-Si : H/μc-Si : H (tandem) modules. The increase in the performance of the CIGS module between the initial and final indoor measurements was approximately 8%. Because of light-induced degradation, the indoor performance of the a-Si : H and a-Si : H/μc-Si : H modules decreased by approximately 35% and 20%, respectively. The performance was improved by about 4–6% under high temperature conditions after the initial degradation. The results suggest that the performance of thin-film silicon modules can seasonally vary by approximately 4–6% only due to thermal annealing and light soaking effects. The effect of solar spectrum enhanced the outdoor performance of the a-Si : H module by about 10% under low air mass conditions, although that of the a-Si : H/μc-Si : H modules showed a little increase. The currents of these a-Si : H/μc-Si : H modules may be limited by the bottom cells. Therefore, it is required to optimize the effect of solar spectrum in addition to the effects of light soaking and thermal annealing, in order to achieve the best performance for thin-film silicon tandem modules.

KEYWORDS

I–V characteristic; metastability; thermal annealing; light soaking; performance ratio (PR); spectral factor (SF)

***Correspondence**

Tetsuyuki Ishii, Research Center for Photovoltaic Technologies, National Institute of Advanced Industrial Science and Technology (AIST), 1-1-1 Umezono, Tsukuba, Ibaraki 305-8568, Japan.
E-mail: tetsuyuki.ishii@aist.go.jp

Received 12 July 2012; Revised 15 October 2012; Accepted 14 November 2012

1. INTRODUCTION

The European Photovoltaic Industry Association (EPIA) has reported that the global solar photovoltaic (PV) installations reached 29.7 GW in 2011 [1]. The investigation of the energy yield and long-term reliability of PV systems is important in order to enhance the "bankability" of PV technologies. Various kinds of PV modules have been developed and commercially available up to present. The performance of PV modules is generally rated under standard test conditions (STC): an irradiance of 1000 W/m^2, an AM1.5G standard spectrum, and a module temperature of 25 °C. However, the performance of thin-film photovoltaic modules is not unique even under STC, because of the "metastability".

The performance of hydrogenated amorphous silicon (a-Si : H) PV modules decreases from the initial performance by light exposure and is recovered by thermal annealing at temperatures above 150 °C. This effect is well known as the Staebler–Wronski effect [2,3]. Copper indium gallium (di)selenide (CIGS) PV modules show an increase in performance with illumination time, the time constant of which is on the order of minutes [4]. Because of the performance change due to thermal annealing and light soaking effects, which have been investigated on the basis of indoor measurements [5–7] and outdoor measurements [8–18],

thin-film PV modules shall be stabilized by light soaking before beginning the measurements defined as IEC 61646 [19]. The quantification of these effects would improve the reliability of the energy rating standard under development and discussion in IEC 61853–3 [20,21]. Some simplified models have applied a sinusoidal function to the seasonal variation of module performance that originated from these effects [22,23].

The time constants of the thermal annealing and light soaking effects of a-Si : H modules are much longer than on the order of hours [5–7,24]. In addition, the performance of a-Si : H modules is sensitive to the change of solar spectrum, because their spectral responses are biased toward shorter wavelength from about 350–800 nm [25–36]. Because of the combination of these effects, complex seasonal variations in performance are shown by a-Si : H modules. Furthermore, tandem PV modules consisting of a-Si : H and hydrogenated micro-crystalline silicon cells (a-Si : H/μc-Si : H), which are prevailing in the markets, show further complex performance variations, because the current is limited by either top or bottom cell under actual outdoor conditions [37–40]. Although it is difficult to develop a general methodology to quantify both the metastability and spectral effects for all commercially available thin-film PV modules, the investigations based on both indoor and outdoor performance measurements are required to achieve the best performance for thin-film PV modules [41,42].

The Research Center for Photovoltaic Technologies, National Institute of Advanced Industrial Science and Technology (AIST) conducted round-robin outdoor measurements, in which the performance of the same PV modules was measured by using the same measurement system at different locations in Japan. The round-robin measurements could be divided into two periods. Polycrystalline silicon (pc-Si) and a-Si : H modules were investigated in the first period from August 2007 to December 2008 [24,34]. The investigation in the second period from October 2008 to December 2009 was focused on the performance of thin-film PV technologies, such as CIGS, a-Si : H, and a-Si : H/μc-Si : H modules. The performance of the thin-film PV modules was measured under outdoor conditions at five locations in Japan, as shown in Figure 1. Figure 2 shows a picture of the measurement system in Okinoerabu. In addition to the outdoor measurements, *I–V* curve measurements under STC were conducted repeatedly using a pulse solar simulator in AIST Tsukuba Center, when we transmitted these modules from one site to another site.

The first purpose of this study is to investigate the change in *I–V* characteristics of thin-film PV modules caused by light soaking and thermal annealing effects. This could be examined by comparing the *I–V* curves obtained by the repeated indoor measurements. The second purpose is to investigate the difference between the outdoor and indoor performance. The difference between the indoor and outdoor performance would reflect the difference in the performance under between STC and actual outdoor conditions.

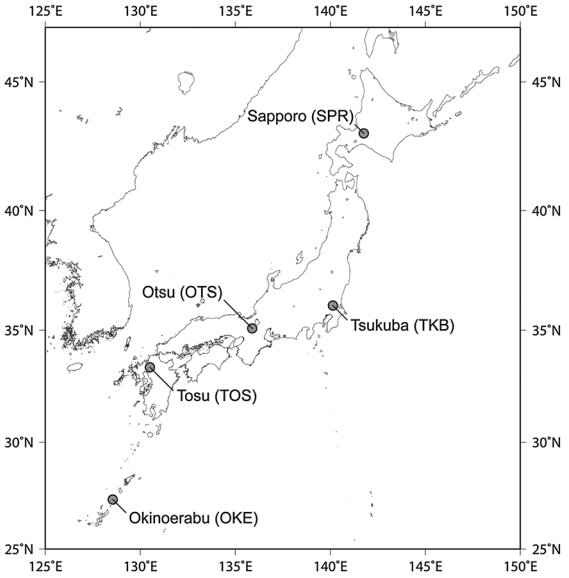

Figure 1. Locations where the round-robin outdoor measurements in the second period were conducted.

2. EXPERIMENTAL METHODS

The performance of six PV modules was investigated in the round-robin measurements in the second period, which was composed of two CIGS (PV07, PV08), one a-Si : H (PV09), and three a-Si : H/μc-Si : H (PV10–PV12) modules. *I–V* curves under outdoor conditions were measured by an *I–V* Curve Tracer, MP-160 (EKO Instruments Co. Ltd, Japan). We also measured solar irradiance, solar spectrum, module temperature, relative humidity, wind speed, and wind direction in this investigation. The outdoor measurement and data collection systems were compiled by CLIMATEC Inc., Japan. A pulse solar simulator, SPI-SUN Simulator™ 1116N (Nisshinbo Mechatronics Inc., Japan) was used for the indoor measurements at AIST Tsukuba Center. The indoor measurements were conducted at transit from one location to another location. Because of the available measurement range for voltage, the CIGS (PV08) module could not be measured by this solar simulator. (Furthermore, this high-voltage CIGS PV module had sometimes stopped the *I–V* Curve Tracer for outdoor measurements. We identified the cause of the missing after the end of the measurements. Therefore, there are many missing values in the outdoor data set.)

We used an EKO/MS-802 pyranometer for solar irradiance measurements. Performance ratio (PR_{OUT}) is used as an indicator of outdoor module performance, which is given by

$$PR_{OUT} = \frac{P_{MAX}}{P_{MAX,\,STC}} \Big/ \frac{G}{G_{STC}} \tag{1}$$

where P_{MAX} is the maximum power output, $P_{MAX,\,STC}$ is the nominal power output defined by the manufacturer, G is the

Figure 2. Picture of the measurement system at the Okinoerabu site (27.21°N, 128.32°E).

solar irradiance, and G_{STC} is the solar irradiance under STC (1 kW/m^2). For solar spectrum measurements, we used two spectroradiometers, EKO/MS-710 and EKO/MS-712 from 350 to 900 nm and from 900 to 1700 nm, respectively. Temperature of each PV module was measured at the center of the back surface by a Type T (copper–constantan) thermocouple. Using the solar spectrum and module temperature, the PR_{OUT} is converted into that under STC ($PR_{OUT,\ STC}$). The conversion equation is given as follows:

$$PR_{OUT,\ STC} = PR_{OUT} \times TF \times SF \tag{2}$$

where TF is the thermal factor and SF is the spectral factor. TF is given by

$$TF = \frac{1}{1 + \gamma(T - T_{STC})} \tag{3}$$

where γ is the maximum power temperature coefficient, T is the module temperature, and T_{STC} is the module temperature under STC (25 °C). SF is given as follows:

$$SF = \frac{\int E_{AM1.5G}(\lambda)SR(\lambda)d\lambda / \int E_{AM1.5G}(\lambda)d\lambda}{\int E(\lambda)SR(\lambda)d\lambda / \int E(\lambda)d\lambda} \tag{4}$$

where $E_{AM1.5G}$ is the standard spectrum defined in IEC 60904-3 [43,44], λ is the wavelength in nanometer, SR is the relative spectral response, and E is the measured solar spectrum. It has been reported that the spectral irradiance measured by spectroradiometers produced by the same manufacturer tends to show a systematical bias [45]. Therefore, the spectroradiometers were recalibrated using a standard lamp [46]. We used solar spectra after the recalibration.

The measurement interval was 5 min. We used only the data measured under fine weather conditions, when solar irradiance was high (more than 750 W/m^2) and stable. The fluctuation of solar irradiance reduced the precision of the measurements, because the measurements of solar irradiance were not perfectly synchronized with the measurements of *I–V* curves. The detailed explanation of data selection for the fine weather conditions is described in [34].

3. RESULTS AND DISCUSSION

3.1. Module temperature in round-robin outdoor measurements

Figure 3 shows the daily mean module temperature of PV07 (CIGS), PV09 (a-Si : H), and PV11 (a-Si : H/μc-Si : H) modules under the high and stable solar irradiance conditions. The temperature of the CIGS module was generally the highest throughout the outdoor measurements. However, the temperature of the CIGS module was exceptionally the lowest during the measurements at the Otsu (OTS) site. This is due to the difference in panel mounting systems. Because of the limitation of space, the CIGS modules (PV07 and PV08) were mounted on open racks, whereas the thin-film silicon modules (PV09–PV12) were mounted on close racks at the Otsu site. Open racks were used for all the other sites. The exceptional use of close racks would result in the high temperature of the thin-film silicon modules at the Otsu site, although the season was spring and the Otsu site was located in the middle of Japan (Figure 1).

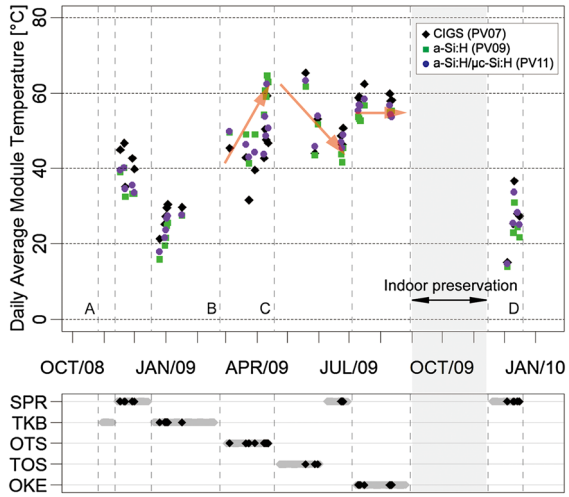

Figure 3. Daily average module temperature under the high and stable solar irradiance conditions. The red arrows indicate the rough trend of the temperature of the thin-film silicon modules. In the lower part, the measured locations are shown by the location codes shown in Figure 1. Grey bars represent the periods when the measurements were conducted. Black dots represent the selected days as fine weather.

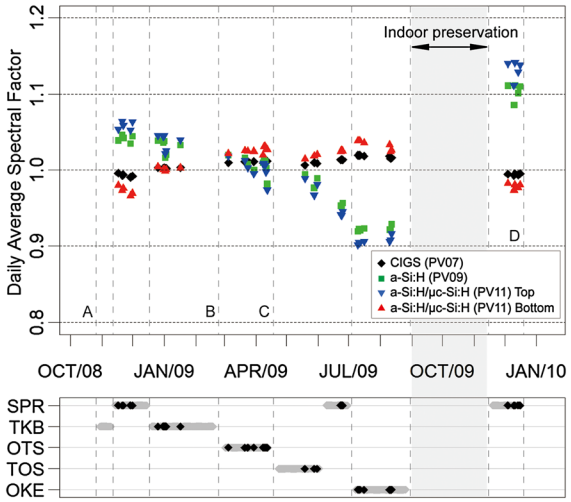

Figure 4. Daily average spectral factor (SF) under the high and stable solar irradiance conditions.

The second measurements in Sapporo (SPR) were conducted during the mid-summer of 2009. However, the Sapporo site was located in the north of Japan (Figure 1). Therefore, the panel temperature was not so high (Figure 3). After the measurements in Sapporo, the PV modules and measurement system were transferred to the Okinoerabu (OKE) site, which was located in the south of Japan. The measurements were conducted during the late summer. Consequently, the module temperature was constantly high. All the PV modules were kept in an indoor environment, where the light level was very low and the ambient temperature was about 25 °C, for two and a half months after the measurements at Okinoerabu. Then, the outdoor measurements were conducted again at the north Sapporo site during winter, where the module temperature was very low.

3.2. Spectral factor (SF)

Solar spectra are strongly influenced by air mass. The difference in latitude between the northernmost site (Sapporo) and southernmost site (Okinoerabu) is about 15.8°. The obliquity of the earth is about 23.4°. The maximum solar altitude changes by about 46.8° between summer and winter solstice. Accordingly, solar spectra were more sensitive to season than location in this investigation. Figure 4 shows the daily mean spectral factor (SF) of the same PV modules shown in Figure 3. Note that the top and bottom cells of the a-Si : H/μc-Si : H modules are described separately. The SF of the CIGS module and μc-Si : H bottom cells was higher in summer (at lower air mass) and lower in winter (at higher air mass). Conversely, the SF of the a-Si : H and a-Si : H top cells was lower in summer and higher in winter. It should be noted that SF less than 1 indicates that the PV performance under STC is lower than that under actual outdoor conditions. Therefore, the performance of the CIGS module and μc-Si : H bottom cells would decrease in summer and would increase in winter by the effect of solar spectrum. Conversely, the performance of the a-Si : H and a-Si : H top cells would increase in summer and would decrease in winter.

3.3. Performance based on indoor measurements

Figure 5 shows the performance ratio (PR_{IN}) based on the indoor measurements, which is the ratio between the power output under STC and nominal power output defined by the manufacturer. We prepared a couple of PV modules for each type: one was preserved in an indoor environment and the other was used for the round-robin outdoor measurements. In order to ascertain the stability of both the solar simulator and preserved modules, the performance of the preserved modules was measured four times, shown as $PR_{IN,\ Preserved}$ in Figure 5. The $PR_{IN,\ Preserved}$ for each module was almost constant. This suggests that the solar simulator was quite stable and that the performance of the thin-film PV modules did not vary in the indoor environment.

The $PR_{IN,\ Exposed}$ represents the performance used for the outdoor measurements based on the indoor measurements. The measurements were conducted nine times for each module. The $PR_{IN,\ Exposed}$ of the CIGS module (PV07) increased by 6.0% after sunlight exposure in Tsukuba (TKB) for about 10 days (Figure 5(a)). The $PR_{IN,\ Exposed}$ slightly increased after the initial increase. The difference in $PR_{IN,\ Exposed}$ between the initial measurement (A) and final measurement (D) was approximately 7.7%. The results

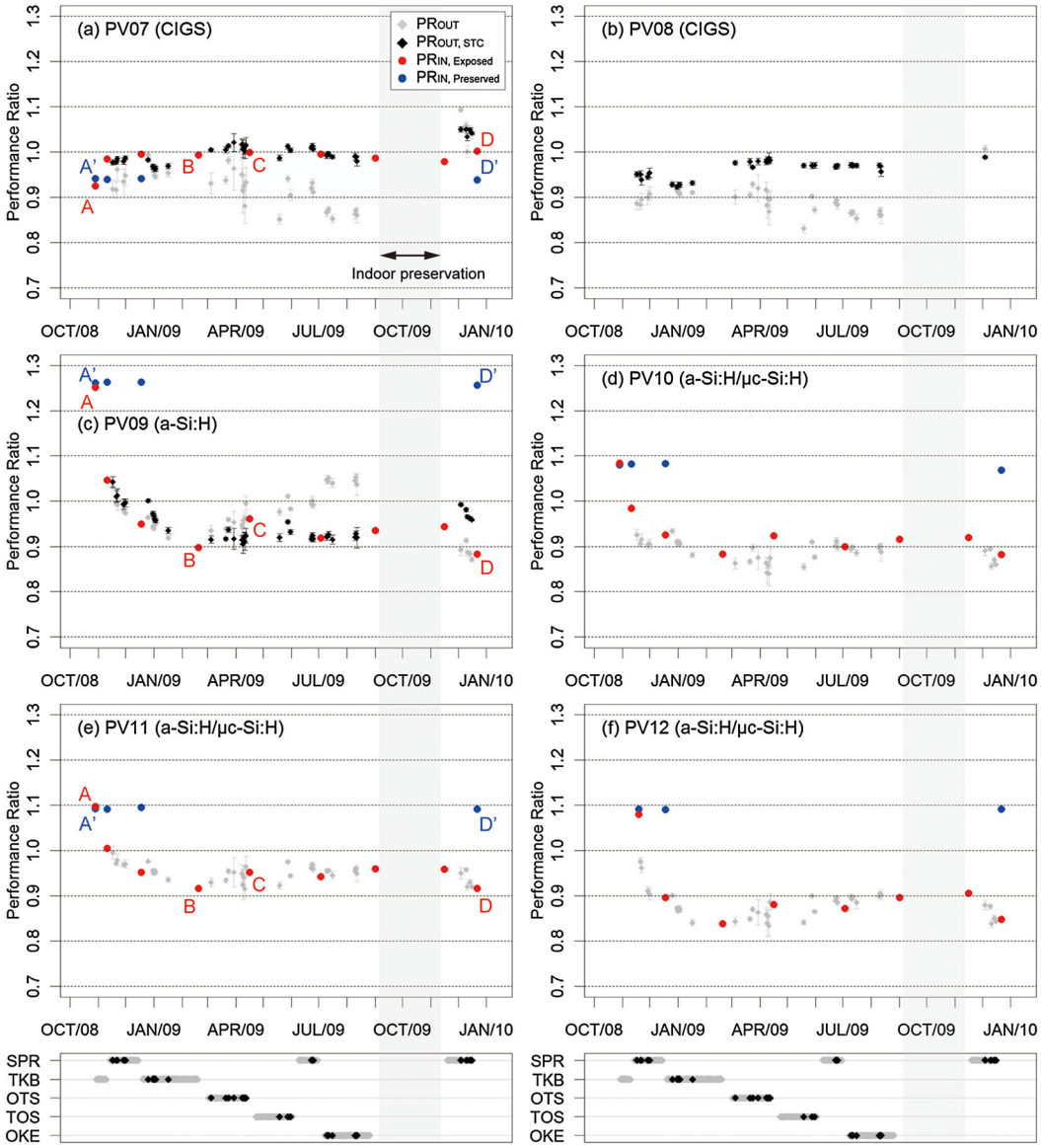

Figure 5. Performance ratio (PR_{OUT}) and PR corrected to STC ($PR_{OUT,\ STC}$) based on the outdoor measurements, in addition to PR of the exposed ($PR_{IN,\ Exposed}$) and PR of the preserved ($PR_{IN,\ Preserved}$) PV modules based on the indoor measurements using a pulse solar simulator under STC. In the lower part, the measured locations are shown by the location codes shown in Figure 1. Grey bars represent the periods when the measurements were conducted. Black dots represent the selected days as fine weather. The alphabets (A–D) correspond to those shown in Figures 3 and 4.

suggest that CIGS module shall be exposed under sunlight for at least 1 month, in order to measure the performance near steady-state conditions.

The $PR_{IN,\ Exposed}$ of the a-Si : H and a-Si : H/μc-Si : H modules (PV09–PV12) shows a similar tendency, although the amplitude of the variation of the a-Si : H module is larger than those of the a-Si : H/μc-Si : H modules (Figure 5(c)–(f)). Because of light-induced degradation, the $PR_{IN,\ Exposed}$ had decreased until the end of 2009 early spring (A–B). The differences in the $PR_{IN,\ Exposed}$ of PV09, PV10, PV11, and PV12 between A and B were approximately 35.5%, 20.0%, 18.2%, and 24.3%, respectively. The $PR_{IN,\ Exposed}$ increased after the outdoor measurements in Otsu, where the module temperature was quite high because the thin-film silicon modules were mounted on close racks as described in Section 3.1. Because the high temperature would enhance the rate of thermal annealing, the $PR_{IN,\ Exposed}$ of these PV modules increased by about 6.4%, 4.1%, 3.6%, and 4.3%, respectively (B–C). The differences in $PR_{IN,\ Exposed}$ between before and after the preservation in an indoor environment for two and a half months were very little, less than 1%. Then, the $PR_{IN,\ Exposed}$ of these modules decreased by

6.0%, 3.8%, 4.2%, and 5.8 %, respectively, during the final outdoor exposure at the Sapporo site (D) in winter. The rate of thermal annealing would be low under the low temperature conditions. These results suggest that the performance of thin-film silicon modules can seasonally vary by several per cent only due to the effects of thermal annealing and light soaking.

3.4. Change in *I–V* characteristics of thin-film PV modules

Figure 6 shows the *I–V* curves of the CIGS, a-Si : H, and a-Si : H/μc-Si : H modules (PV07, PV09, and PV11) measured by the solar simulator under STC. The *I–V* curves of the preserved modules, which were measured four times for each module, are almost perfectly overlapped (Figure 6(d)–(f)). The results suggest that the solar simulator had been quite stable. Figure 6(a)–(c) shows the *I–V* curves of the modules for outdoor exposure, the measurements of which were conducted nine times at transit from one location to another location. The light-induced improvement in the performance of the CIGS module is mainly due to the increase in fill factor (FF) as shown in Figure 6a. The open circuit voltage (V_{oc}) slightly increases with increasing the module performance. Conversely, the short circuit current (I_{sc}) slightly decreases with increasing the module performance. The main factor of the light-induced performance variation of the thin-film silicon modules is the decrease or increase in FF as shown in Figure 6(b) and (c). Both the V_{oc} and I_{sc} slightly decrease with decreasing the module performance.

3.5. Performance based on outdoor measurements

Figure 5 shows the performance ratio under outdoor conditions (PR_{OUT}) calculated from Equation (1) and the performance ratio corrected to STC ($PR_{OUT,\ STC}$) based on Equation (2). The error bars represent the standard deviations (1σ), indicating the daily dispersion of PR_{OUT} and $PR_{OUT,\ STC}$. In this study, we could not correct the PR_{OUT} of the a-Si : H/μc-Si : H modules to STC, because we could not identify whether the current was limited by the top or bottom cell. Therefore, only the PR_{OUT} is shown in Figure 5(d)–(f). The temperature coefficients (γ) of the CIGS and a-Si : H modules in Equation (3) is assumed to be −0.33% and +0.12%, respectively. We refer to the manufacturer's specification for the temperature coefficient of the CIGS modules. The temperature coefficients of a-Si : H modules in short timescale such as hours before reaching steady-state conditions are negative values. However, the apparent temperature coefficients in long timescale such as days after reaching near steady-state conditions are positive

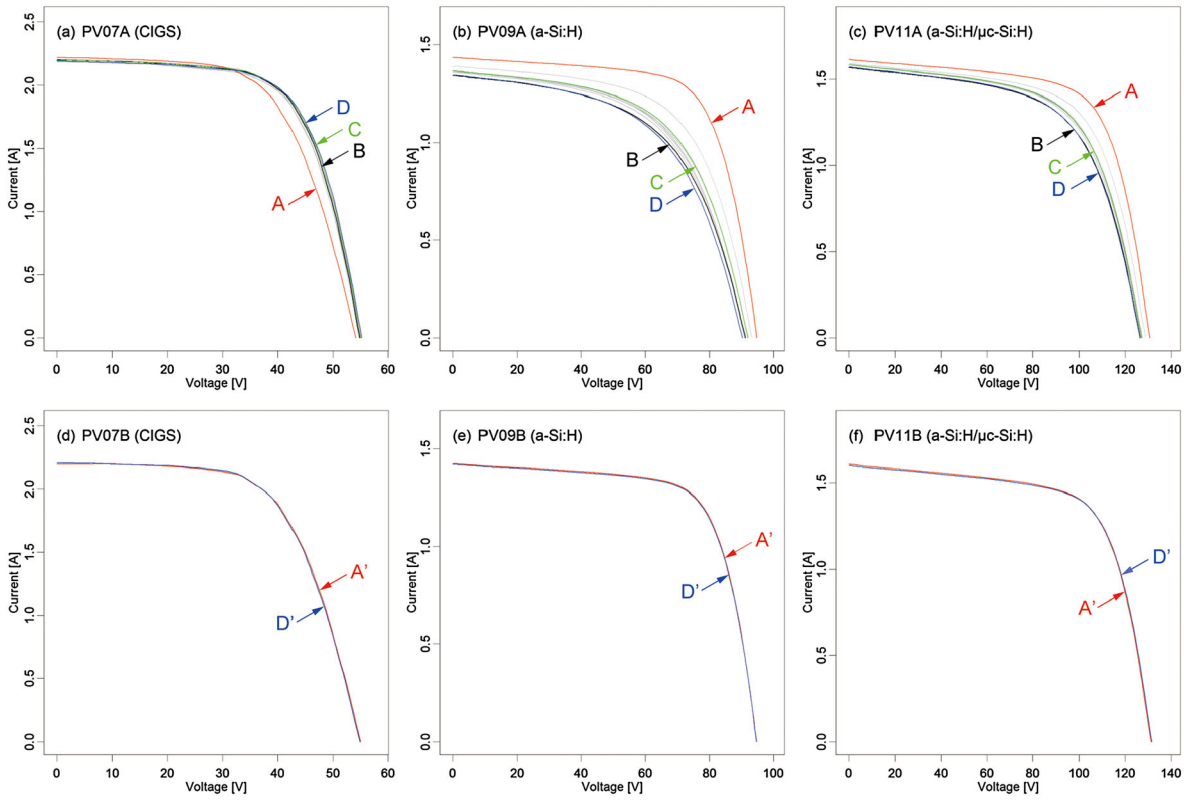

Figure 6. *I–V* curves of the exposed modules (a–c) and the preserved modules (d–f) based on the indoor measurements under STC. The alphabets (A-D, A′, and D′) correspond to those shown in Figure 5.

values, because of the combination of the inherent temperature coefficient and metastable (thermal annealing and light soaking) effects [24,47]. The positive value of +0.12% in long timescale in [24] is adopted in this study.

The $PR_{OUT,\ STC}$ of the CIGS module was almost equal to the $PR_{IN,\ Exposed}$, whereas the $PR_{OUT,\ STC}$ fluctuated by about ±5% among the locations (Figure 5(a)). Therefore, we can ignore the effect of light soaking when estimating the power or energy output of CIGS modules, if the CIGS modules are adequately exposed to sunlight.

The pattern of changes in the $PR_{IN,\ Exposed}$ of the a-Si : H module is similar to those of the a-Si : H/μc-Si : H modules (Figure 5(c)–(f)). However, the pattern of changes in the PR_{OUT} is different between the a-Si : H and a-Si : H/μc-Si : H modules. The PR_{OUT} of the a-Si : H module largely increased in summer (Figure 5(c)). In particular, the PR_{OUT} was more than 10% larger than the $PR_{IN,\ Exposed}$ in Okinoerabu. The SF of the a-Si : H module in Okinoerabu was about 0.9 (Figure 4), indicating the performance increased by about 10% due to the effect of solar spectrum. However, the PR_{OUT} of the a-Si : H/μc-Si : H modules showed a little increase in summer, which was almost equal to the $PR_{IN,\ Exposed}$ (Figure 5(d)–(f)). The top cell of an individual multijunction cell in an a-Si : H/μc-Si : H device is connected in series to the bottom of the adjacent individual multijunction cell. The SF of the bottom cells was much higher than that of the top cells at the Okinoerabu site in late summer (Figure 4). The results may be interpreted that the currents of these a-Si : H/μc-Si : H modules were limited by the currents of the bottom cells. Therefore, it is required to optimize the effect of solar spectrum in addition to the effects of light soaking and thermal annealing, in order to achieve the best performance for thin-film silicon tandem modules.

4. CONCLUSIONS

The metastability of thin-film PV modules was investigated on the basis of both the indoor measurements and outdoor round-robin measurements in Japan. The investigated thin-film PV modules were CIGS, a-Si : H, and a-Si : H/μc-Si : H tandem modules. The change in *I–V* characteristics of the thin-film PV modules induced by light soaking and thermal annealing effects was examined by the repeated indoor measurements using the solar simulator in AIST. The light-induced improvement in the performance of the CIGS module was mainly due to the increase in FF. Also, the main factor of the light-induced performance variation of the thin-film silicon modules was the decrease or increase in FF.

The $PR_{IN,\ Exposed}$ of the CIGS module increased by 6% after the initial sunlight exposure in Tsukuba for about 10 days. The difference in $PR_{IN,\ Exposed}$ between the initial and final indoor measurements was approximately 8%. Consequently, CISG modules are likely to require outdoor sunlight exposure for about 1 month to reach near steady-state conditions. The nominal performance under STC shall be measured just after the adequate sunlight exposure. The $PR_{OUT,\ STC}$ shows good agreement with the $PR_{IN,\ Exposed}$ of the CIGS module.

Due to light-induced degradation, the $PR_{IN,\ Exposed}$ of the a-Si : H and a-Si : H/μc-Si : H modules decreased by approximately 35% and 20%, respectively. After the degradation, the $PR_{IN,\ Exposed}$ of these modules improved by about 4–6%, because of the enhancement in the rate of thermal annealing under high temperature conditions in Otsu. The $PR_{IN,\ Exposed}$ decreased by approximately 4–6% after the final outdoor exposure under low temperature conditions in Sapporo. The results suggest that the performance of thin-film silicon modules can seasonally vary by about 4–6% only because of thermal annealing and light soaking effects. The effect of solar spectrum enhanced the PR_{OUT} of the a-Si : H module by about 10% at the Okinoerabu site in late summer, although the PR_{OUT} of the a-Si : H/μc-Si : H modules showed a little increase. The performance of the a-Si : H/μc-Si : H modules may be limited by the currents of the bottom cells.

ACKNOWLEDGEMENTS

This study was financially supported by the New Energy and Industrial Technology Development Organization (NEDO) under the Ministry of Economy, Trade and Industry (METI).

REFERENCES

1. The European Photovoltaic Industry Association (EPIA). 2011 annual report. 2011.
2. Staebler DL, Wronski CR. Reversible conductivity changes in discharge-produced amorphous Si. *Applied Physics Letters* 1977; **31**(4): 292–294.
3. Staebler DL, Wronski CR. Optically induced conductivity changes in discharge-produced hydrogenated amorphous silicon. *Journal of Applied Physics* 1980; **51**(6): 3262–3268.
4. Ruberto MN, Rothwarf A. Time-dependent open-circuit voltage in $CuInSe_2$/CdS solar cells: theory and experiment. *Journal of Applied Physics* 1986; **61**(9): 4662–4669.
5. Takahisa K, Kojima T, Nakamura K, Koyanagi T, Yanagisawa T. Experimental model and long-term prediction of photovoltaic conversion efficiency of a-Si solar cells. *Solar Energy Materials and Solar Cells* 1997; **49**(1–4): 179–186.
6. del Cueto JA, von Roedern B. Temperature-induced changes in the performance of amorphous silicon multi-junction modules in controlled light soaking. *Progress in Photovoltaics: Research and Applications* 1999; **7**(2): 101–112.
7. Korostyshevsky A, Hausgen PE, Granata JE, Sahlstrom TD. Temperature dependence of light-induced degradation

in amorphous silicon solar cells. *Proceedings of the 31st IEEE Photovoltaic Specialists Conference*, Orlando, USA, 2005, 1532–1535. DOI: 10.1109/PVSC.2005.1488435
8. Costa HS, Ragot Ph, Desmettre D. Evaluation of amorphous silicon module outdoor performances. *Solar Energy Materials and Solar Cells* 1992; **27**(1): 59–68.
9. Rüther R, Livingstone J. Seasonal variations in amorphous silicon solar module outputs and thin film characteristics. *Solar Energy Materials and Solar Cells* 1994; **36**(1): 29–43.
10. Strand T, Mrig L, Hansen R, Emery K. Technical evaluation of a dual-junction same-band-gap amorphous silicon photovoltaic system. *Solar Energy Materials and Solar Cells* 1996; **41/42**: 617–628.
11. Akhmad K, Kitamura A, Yamamoto F, Okamoto H, Takakura H, Hamakawa Y. Outdoor performance of amorphous silicon and polycrystalline silicon PV modules. *Solar Energy Materials and Solar Cells* 1997; **46**(3): 209–218.
12. Ikisawa M, Nakano A, Igari S, Terashima H. Outdoor exposure tests of photovoltaic modules in Japan and overseas. *Renewable Energy* 1998; **14**(1–4): 95–100.
13. Merten J, Andreu J. Clear separation of seasonal effects on the performance of amorphous silicon solar modules by outdoor I/V measurements. *Solar Energy Materials and Solar Cells* 1998; **52**(1–2): 11–25.
14. King DL, Kratochvil JA, Boyson WE. Stabilization and performance characteristics of commercial amorphous-silicon PV modules. *Proceedings of the 28th IEEE Photovoltaic Specialists Conference*, Alaska, USA, 2000, 1446–1449. DOI: 10.1109/PVSC.2000.916165
15. Carr AJ, Pryor TL. A comparison of the performance of different PV module types in temperate climates. *Solar Energy* 2004; **76**(1–3): 285–294. DOI: 10.1016/j.solener.2003.07.026
16. Rüther R, Tamizh-Mani G, del Cueto J, Adelstein J, Dacoregio MM, von Roedern B. Performance test of amorphous silicon modules in different climates—year three: higher minimum operating temperatures lead to higher performance levels. *Proceedings of the 31st IEEE Photovoltaic Specialists Conference*, Florida, USA, 2005, 1635–1638. DOI: 10.1109/PVSC.2005.1488459
17. Nakada Y, Fukushige S, Minemoto T, Takakura H. Seasonal variation analysis of the outdoor performance of amorphous Si photovoltaic modules using the contour map. *Solar Energy Materials and Solar Cells* 2009; **93**(3): 334–337. DOI: 10.1016/j.solmat.2008.11.011
18. Fukushige S, Ichida K, Minemoto T, Takakura H. Analysis of the temperature history of amorphous silicon photovoltaic modules outdoors. *Solar Energy Materials and Solar Cells* 2009; **93**(6–7): 926–931. DOI: 10.1016/j.solmat.2008.11.009
19. International Electrotechnical Commission. Thin-film terrestrial photovoltaic (PV) modules—design qualification and type approval. *IEC 61646 Edition 2.0*, 2008.
20. International Electrotechnical Commission. Photovoltaic (PV) module performance testing and energy rating—part 3: energy rating of PV modules. *IEC 61853–3 Working Draft*, 2011.
21. Kenny RP, Dunlop ED, Ossenbrink HA, Müllejans H. A practical method for the energy rating of c-Si photovoltaic modules based on standard tests. *Progress in Photovoltaics: Research and Applications* 2006; **14**(2): 155–166. DOI: 10.1002/pip.658
22. Akhmad K, Okamoto H, Yamamoto F, Kitamura A. Long-term performance modelling of amorphous silicon photovoltaic module. *Japanese Journal of Applied Physics* 1997; **36**(2): 629–632.
23. Nikolaeva-Dimitrova M, Kenny RP, Dunlop ED, Pravettoni M. Seasonal variations on energy yield of a-Si, hybrid, and crystalline Si PV modules. *Progress in Photovoltaics: Research and Applications* 2010; **18**(5): 311–320. DOI: 10.1002/pip.918
24. Ishii T, Otani K, Takashima T, Kawai S. Estimation of the maximum power temperature coefficients of PV modules at different time scales. *Solar Energy Materials and Solar Cells* 2011; **95**(1): 386–389. DOI: 10.1016/j.solmat.2010.04.041
25. Wilson HR, Hennies M. Energetic relevance of solar spectral variation on solar cell short circuit current. *Solar Energy* 1989; **42**(3): 273–279.
26. Nann S, Emery K. Spectral effects on PV-device rating. *Solar Energy Materials and Solar Cells* 1992; **27**(3): 189–216.
27. Hirata Y, Tani T. Output variation of photovoltaic modules with environmental factors: I. The effect of spectral solar radiation on photovoltaic module output. *Solar Energy* 1995; **55**(6): 463–468.
28. Gottschalg R, Infield DG, Kearney MJ. Experimental study of variations of the solar spectrum of relevance to thin film solar cells. *Solar Energy Materials and Solar Cells* 2003; **79**(4): 527–537.
29. Nakajima A, Ichikawa M, Kondo M, Yamamoto K, Yamagishi H, Towada Y. Spectral effects of a single-junction amorphous silicon solar cell on outdoor performance. *Japanese Journal of Applied Physics* 2004; **43**(5A): 2425–2431. DOI: 10.1143/JJAP.43.2425
30. Müllejans H, Ioannides A, Kenny R, Zaaiman W, Ossenbrink H, Dunlop E. Spectral mismatch in calibration of photovoltaic reference devices by global sunlight method. *Measurement Science and Technology* 2005; **16**(6): 1250–1254. DOI: 10.1088/0957-0233/16/6/002

31. Kenny RP, Ioannides A, Müllejans H, Zaaiman W, Dunlop ED. Performance of thin film PV modules. *Thin Solid Films* 2006; **511-512**(26): 663–672. DOI: 10.1016/j.tsf.2005.11.066
32. Pérez-López JJ, Fabero F, Chenlo F. Experimental solar spectral irradiance until 2500 nm: results and influence on the PV conversion of different materials. *Progress in Photovoltaics: Research and Applications* 2007; **15**(4): 303–315. DOI: 10.1002/pip.739
33. Tsutsui J, Kurokawa K. Investigation to estimate the short circuit current by applying the solar spectrum. *Progress in Photovoltaics: Research and Applications* 2008; **16**(3): 205–211. DOI: 10.1002/pip.793
34. Ishii T, Otani K, Takashima T. Effects of solar spectrum and module temperature on outdoor performance of photovoltaic modules in round-robin measurements in Japan. *Progress in Photovoltaics: Research and Applications* 2011; **19**(2): 141–148. DOI: 10.1002/pip.995
35. Monokroussos C, Bliss M, Qiu YN, Hibberd CJ, Betts TR, Tiwari AN, Gottschalg R. Effects of spectrum on the power rating of amorphous silicon photovoltaic devices. *Progress in Photovoltaics: Research and Applications* 2011; **19**(6): 640–648. DOI: 10.1002/pip.1080
36. Ishii T, Otani K, Itagaki A, Utsunomiya K. A methodology for estimating the effect of solar spectrum on photovoltaic module performance by using average photon energy and a water absorption band. *Japanese Journal of Applied Physics* 2012; **51**(10): 10NF05. DOI: 10.1143/JJAP.51.10NF05
37. Gottschalg R, Betts TR, Infield DG, Kearney MJ. The effect of spectral variations on the performance parameters of single and double junction amorphous silicon solar cells. *Solar Energy Materials and Solar Cells* 2005; **85**(3): 415–428. DOI: 10.1016/j.solmat.2004.05.011
38. Nakajima A, Gotoh M, Sawada T, Fukuda S, Yoshimi M, Yamamoto K, Nomura T. Development of thin-film Si HYBRID solar module. *Solar Energy Materials and Solar Cells* 2009; **93**(6–7): 1163–1166. DOI: 10.1016/j.solmat.2009.03.006
39. Sutterlueti J, Kravets R, Keller M, Knauss H, Sinicco I, Huegli A. Energy yield optimization and seasonal behavior of Micromorph® thin film modules. *Proceedings of the 25th European Photovoltaic Solar Energy Conference and Exhibition / 5th World Conference on Photovoltaic Energy Conversion*, Valencia, Spain, 2010, 4269–4275. DOI: 10.4229/25thEUPVSEC2010-4AV.3.88
40. Ishii T, Otani K, Takashima T, Xue Y. Solar spectral influence on the performance of photovoltaic (PV) modules under fine weather and cloudy weather conditions. *Progress in Photovoltaics: Research and Applications* 2013; available online. DOI: 10.1002/pip.1210
41. Nikolaeva-Dimitrova M, Kenny RP, Dunlop ED. Controlled conditioning of a-Si : H thin film modules for efficiency prediction. *Thin Solid Films* 2008; **516**(20): 6902–6906. DOI: 10.1016/j.tsf.2007.12.059
42. Virtuani A, Müllejans H, Dunlop ED. Comparison of indoor and outdoor performance measurements of recent commercially available solar modules. *Progress in Photovoltaics: Research and Applications* 2011; **19**(1): 11–20. DOI: 10.1002/pip.977
43. International Electrotechnical Commission. Photovoltaic devices—part 3: measurement principles for terrestrial photovoltaic (PV) solar devices with reference spectral irradiance data. *IEC 60904–3 Edition 2.0*, 2008.
44. Gueymard CA. Parameterized transmittance model for direct beam and circumsolar spectral irradiance. *Solar Energy* 2001; **71**(5): 325–346.
45. Krawczynski M, Strobel MB, Gottschalg R. Intercomparison of spectroradiometers for outdoor performance monitoring. *Proceedings of the 24th European Photovoltaic Solar Energy Conference and Exhibition*. Hamburg, Germany, 2009, 3406–3408. DOI: 10.4229/24thEUPVSEC2009-4AV.3.37
46. Xue Y, Otani K, Tsuno Y, Hishikawa Y. Evaluation of spectroradiometers for outdoor photovoltaic module performance monitoring. *Proceedings of Renewable Energy 2010*. Yokohama, Japan, 2010, O-Pv-8-4.
47. Ishii T, Takashima T, Otani K. Long-term performance degradation of various kinds of photovoltaic modules under moderate climatic conditions. *Progress in Photovoltaics: Research and Applications* 2011; **19**(2): 170–179. DOI:10.1002/pip.1005